Intelligent coverage path planning for agricultural robots and autonomous machines on three-dimensional terrain

Hameed, Ibahim

Published in:
Journal of Intelligent and Robotic Systems

DOI (link to publication from Publisher):
10.1007/s10846-013-9834-6

Publication date:
2014

Document Version
Publisher's PDF, also known as Version of record

J Intell Robot Syst (2014) 74:965–983
DOI 10.1007/s10846-013-9834-6

Intelligent Coverage Path Planning for Agricultural Robots and Autonomous Machines on Three-Dimensional Terrain

I. A. Hameed

Received: 21 September 2012 / Accepted: 22 April 2013 / Published online: 4 May 2013

Abstract Field operations should be done in a manner that minimizes time and travels over the field surface. Automated and intelligent path planning can help to find the best coverage path so that costs of various field operations can be minimized. The algorithms for generating an optimized field coverage pattern for a given 2D field has been investigated and reported. However, a great proportion of farms have rolling terrains, which have a considerable influence on the design of coverage paths. Coverage path planning in 3D space has a great potential to further optimize field operations and provide more precise navigation. Supplementary to that, energy consumption models were invoked taking into account terrain inclinations in order to provide the optimal driving direction for traversing the parallel field-work tracks and the optimal sequence for handling these tracks under the criterion of minimizing direct energy requirements. The reduced energy requirements and consequently the reduced emissions of atmospheric pollutants, e.g. CO_2 and NO, are of major concern due to their contribution to the greenhouse effect. Based on the results from two case study fields, it was shown that the reduction in the energy requirements when the driving angle is optimized by taking into account the 3D field terrain was 6.5 % as an average for all the examined scenarios compared to the case when the applied driving angle is optimized assuming even field terrain. Additional reduction is achieved when sequence of field tracks is optimized by taking into account inclinations for driving up and down steep hills.

Keywords Route planning · DEM · Optimization · Genetic algorithm

I. A. Hameed (✉)
Faculty of Engineering and Science,
Department of Electronic Systems,
Aalborg University, Fredrik Bajers Vej 7B,
9220, Aalborg, Denmark
e-mail: ih@es.aau.dk,
ibrahimabdelhameed@yahoo.com

1 Introduction

Around 36 % of direct energy use in agriculture is gas oil/diesel for field operations. The largest users are the arable crop sectors (66 %), the dairy, beef and sheep sectors use an additional 31 % and the horticultural field crops sector uses 3 %. Savings can be made by the producers themselves by correct tractor ballasting, tyre selection and implement matching but it is thought unlikely that these measures have the potential to save more than 10 % of the total fuel used [15]. According to a Food and Agriculture Organization (FAO), the food sector around the globe has an over dependence on fossil fuels that may limit the sector's

ability to meet global food demands. With the high and fluctuating prices of fossil fuels there is a need for new strategies. Several recommendations were suggested in every step of food production such as the use of more efficient engines and improving energy efficiency [2]. In addition to the economic impact of the reduced energy consumption in field operations, the agricultural vehicles used in various field work activities emit significant levels of atmospheric pollutants, which include carbon dioxide (CO_2) and nitrogen oxide (NO), both of which are of major concern due to their contribution to the greenhouse effect. Reducing pollutant outputs through reduced fuel consumption therefore yield both environmental and financial benefits [14].

Fuel consumption may be reduced by developing optimized in-field coverage planning for agricultural machines. Recently, a number of automated coverage planning algorithms have been developed for the optimization and automation of autonomous field operations. For example, Oksanen and Visala [11] and Jin and Tang [9] developed algorithmic approaches to find efficient 2D coverage paths involving field area decomposition in sub-regions and optimal driving line direction. Hameed et al. [6] presented a fully automated 2D coverage path planning approach which is able to cover any field regardless of its shape complexity with the option of using a user-defined driving angle or by driving parallel to the longest edge of the field as the optimal driving direction. Bochtis and Vougioukas [1] presented the algorithmically-computed optimal fieldwork patterns, the B-patterns, which provide the optimal field-work track sequencing according to the criterion of the minimization of the non-working travelled distance of an agricultural vehicle. Hameed et al. [4] derived a genetic algorithm based approach for the simultaneous selection of the driving direction and the sequence of tracks that minimizes operational time and overlapped area. Hameed et al. [5] developed a genetic algorithm based coverage path planning approach for covering fields with obstacle areas by clustering the field tracks into independent blocks and finding the optimum sequence of blocks in a manner which minimizes the connection distance between blocks.

A critical factor, however, that has not been taken into account in the above studies is the effect attributed to varying terrain conditions. The rolling terrains of many farms have considerable influence on the design of coverage paths: only 47 % of cropland in the United States is only less than 2 % slopes; 48 % of the cropland is on slopes between 2 % and 10 %. Therefore, coverage path planning for three dimensional (3D) terrain fields has a great potential for further optimizing field operations [12]. Only limited research on developing area coverage planning for 3D terrain has been reported. For example, Jin and Tang [10] developed an optimized 3D terrain field coverage path planning algorithm that classifies the field terrain into flat and sloppy areas and then applies the most appropriate path planning strategy to each region in terms of minimized headland turning cost, soil erosion cost, and skipped/overlapped area cost. Hameed et al. [8] developed a coverage path planning method for agricultural vehicles carrying time-depended loads over 3D terrain with the objective of reducing energy consumption by finding the best driving direction. The terrain characteristics are expected to have significant influence on the design and optimization of the coverage path planning. Especially in terms of elevation variations, elevation changes, or slopes have considerable influence on soil erosion, skips and overlaps between furrows, and vehicle's fuel consumption [10].

Material handling operations with time-depending loads carried by the agricultural vehicles specifically presents a potential for saving direct energy consumption in elevated terrains by optimizing the relation between the inclination of a specific part of the area, the driving direction, and the load carried by the vehicle while operating on this part. These operations involve traversing the field with varying loads depending on the emptying or state of the carrying unit. The capacity constraints require that the vehicle has to execute a number of routes with varying loads in order to complete the operation (e.g., harvesting and fertilizing) [8].

The objective of this paper is to develop and implement a 3D coverage planning approach for material input operations that minimizes the energy requirements. The approach will be based on

developed tools for 2D geometrical representation and expanded to a 3D representation, and a simulation tool for field operations under capacity constraints. The approach will be supplemented with energy consumption models taking into account terrain inclinations in order to provide the optimal driving line direction for traversing the parallel field-work tracks under the criterion of minimized direct energy requirements. In addition, a further reduction in fuel consumption is achieved through the use of an integer-valued genetic algorithm to find the best sequence of field-work tracks that enable an agriculture machine or a robot to drive up and down steep hills using the minimum fuel consumption.

2 Methodology

2.1 General

The approach provides, for a given field and given machinery characteristics, the optimal driving direction and/or the optimal sequence for traversing the parallel field-work tracks in terms of minimized direct energy requirements. This process can be carried out in two different ways as follows.

2.1.1 2D/3D Genetic Algorithm Based Approach

The decision variables of this optimization problem are the driving angle, which is defined as the angle between the driving line direction and the horizontal axis of the applied Euclidean coordinates system, and the sequence of field tracks. The method is divided into two levels. At the first level, nonworking in-field travelled distance cost and hence the total field operational time is minimized. An existing 2D field representation generation tool (described in Section 2.2) is applied and a genetic algorithm (GA) is used to find the best possible driving angle which enables an agriculture machine or a robot to cover the field area using the minimum number of field tracks and hence the minimum headland turning cost. Headland turning cost is defined as the distance travelled over headland area in turnings which can be further reduced by using simple turning types which does not require complex maneuvering over headland area. In this level, the optimization process takes place using the 2D field representation since elevation does not appear in the governing equations used for calculating turning distance over headland area [4]. At the second level of the optimization process, the generated 2D field representation for the optimized driving angle is combined with the information provided by the digital elevation model (DEM) of the field area to generate the 3D representation of the field under consideration. A fuel consumption models (described in Section 2.5) are used for estimating the direct energy requirements for the execution of the operation by driving through each single track from one end to the other end and vice versa. Fuel consumption is estimated in terms of the percentage gradient of the vehicle's route and therefore there is always a difference in fuel consumption depending on the direction the vehicle used to enter each track. The optimal entrance directions for all the field tracks are then obtained and the best sequence of tracks is obtained in such a way to enable a vehicle to cover all tracks with the minimum headland turning cost and the minimum possible fuel consumption. To sum up, the main task of the second level of this process is to further optimize the fuel consumption by finding the best sequence of tracks that can use the less gradient routes to drive up the field's steep hills. A flowchart of the proposed optimization approach is shown in Fig. 1.

2.1.2 3D Exhaustive Search Approach

As a decision variable of the optimization problem is considered the driving angle, which is defined as the angle between the driving line direction and the horizontal axis of the applied Euclidean coordinates system. The method is based on an exhaustive search among all possible integer values of driving angles between 1° and 180°. The stages involved in the search are described in Fig. 2. In the first stage an existing 2D field representation generation tool (described in Section 2.2) is applied. In a next stage (described in Section 2.3), by combining the generated 2D representation and the information provided by the digital elevation model (DEM) of the field, a

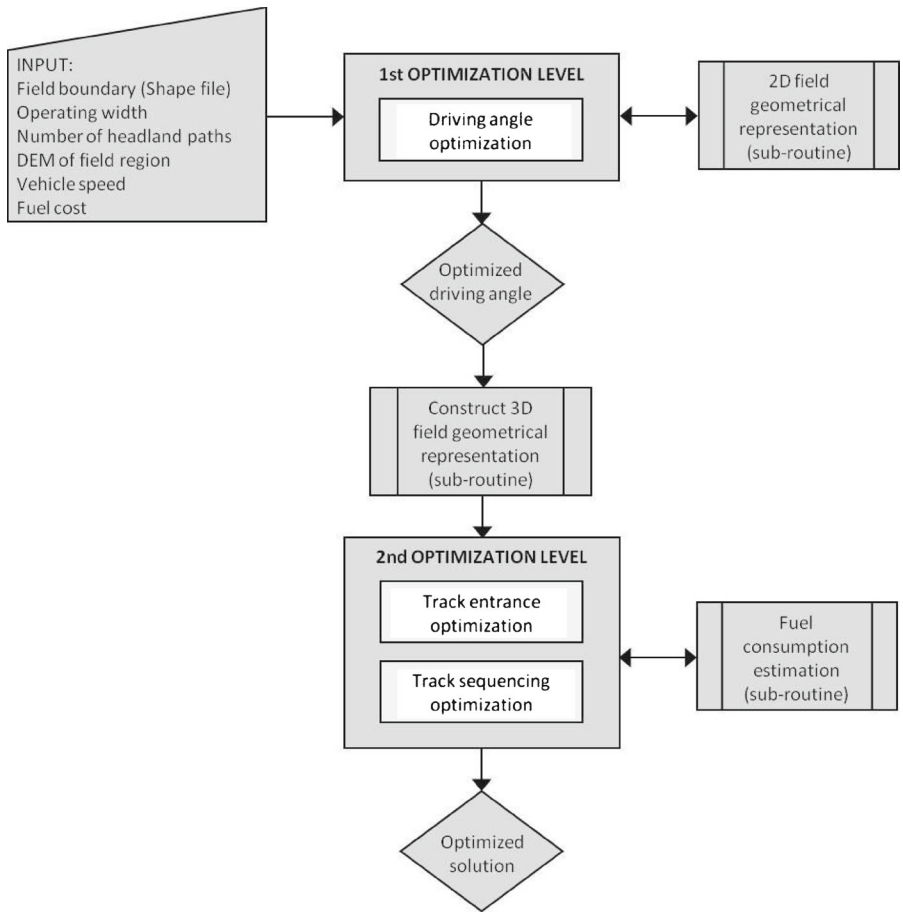

Fig. 1 Flowchart of the 2D/3D GA-based optimization approach

3D representation is generated. Then an existing simulation tool for input material handling operations with capacity constraints is applied (described in Section 2.4). The simulation provides the path followed by the agricultural vehicle for a complete field coverage and the corresponding carried load in each way-point. In the last stage, using fuel consumption models (described in Section 2.5), the total direct energy requirements for the execution of the operation using the tested driving angle are estimated. The tested driving angle with the minimum estimated direct energy requirements is selected as the optimal one.

2.2 2D Field Representation

For the 2D geometrical representation of the field, a tool developed by [6] was used. The 2D geometrical representation of a field involves the generation of a geometrical map which is made divided into discrete geometric primitives, such as points, lines, and polygons; providing a concise representation of the environmental data that can be readily used for operational planning. The input consists of the set of coordinates of the points on the field boundary, the operating width of the implement, the number of headland paths, and the tested driving direction. The tool generates the set of the parallel field-work tracks for the complete field area coverage and gives as an output of the coordinates of the points representing the starting and the ending point of each track, and of the points representing the headland paths (Fig. 3). The tool was implemented using the MATLAB® technical programming language.

2.3 3D Terrain Representation

In this stage, the 2D field representation is converted into a 3D field representation. The

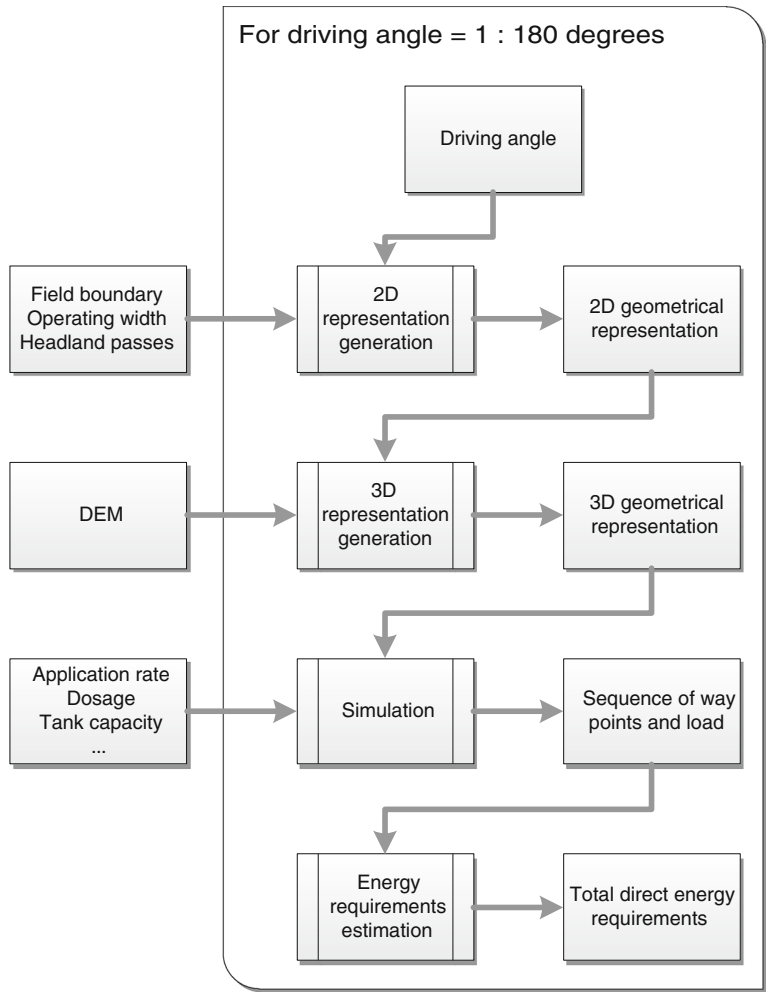

Fig. 2 Flowchart of the 3D exhaustive search optimization approach

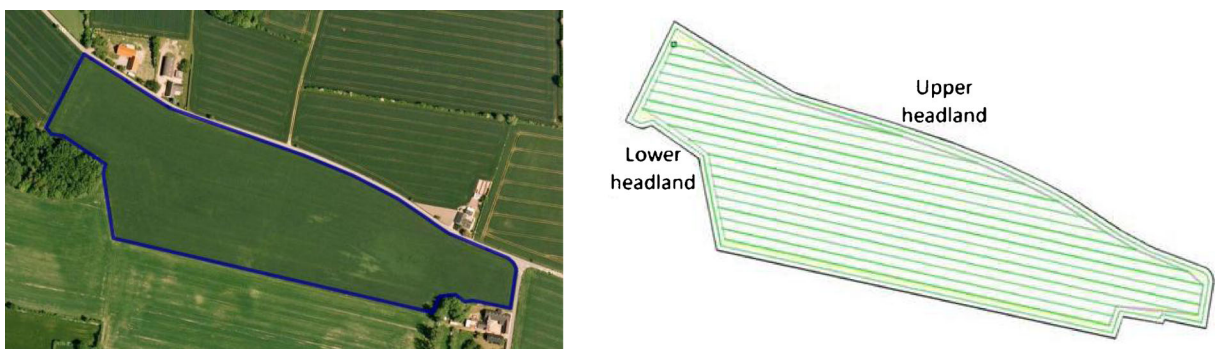

(a) (b)

Fig. 3 Example implementation of the 2D geometrical field representation: **a** Satellite image of a field (55° 32′ 10.00″ N, 10° 4′ 1.96″ E) with the outer field boundary in blue **b** The geometrical representation of the field for an operating width of 9 m, a driving angle of −12.5°, and a single headland path

information regarding the field topography needed for the generation of a 3D representation of the field terrain is provided by a digital file, called digital elevation model (DEM), consisting of terrain elevation for ground positions at regularly spaced horizontal intervals. DEM's data are structured as a grid of squares or cells [13]. The cell length (m) represents the accuracy of the terrain representation in 3D space and this value is defined in the DEM file. A DEM file is arranged as an ASCI grid file containing, in its header, the file id, cell length, number of grid lines along x-axis, number of grid lines along y-axis, minimum and maximum x values of the grid in UTM, minimum and maximum y value of the grid in UTM, and minimum and maximum elevation values of the grid in UTM. Then elevation values of the grid cells (i.e., z values) are ordered in rows in the rest of the file representing the elevation matrix. The cell length of the field examples used in this paper is 1.6 m.

The 3D representation of the field is obtained by dividing each line segment of the 2D field representation into small segments each of a length less than or equal to the cell length of the elevation model (i.e., DEM file) of the field area. After division, each resultant segment has two waypoints, namely, starting and ending points in 2D space. A unique cell from the DEM file is then allocated to each resultant waypoint and the elevation of each matched cell is assigned to its relevant waypoint of the 2D representation. A search sub-routine is used to allocate each waypoint of the 2D representation to a DEM cell. A pseudo-code of the developed search sub-routine is given in Table 1 for converting a 2D field-work track into the corresponding 3D representation.

Table 1 Elevation search pseudo-code

```
READ elevationMatrix, xmax, xmin, ymax, ymin, cellLength FROM DEM
x =[xmax : -cellLength : xmin]
y =[ymax : -cellLength : ymin]
FOR each track (or headland path) segment
       READ segmentStarPoint, segmentEndPoint
       DEFINE stepSize = cellLength
       segmentLine = CREATELINE(segmentStarPoint,  segmentEndPoint)
       segmentLength = LENGTH(segmentLine)
       numberOfCells = ROUND(segmentLength/cellLength)
       WHILE numberOfCells > 0
          [xp, yp] = POINTONLINE(segmentLine, stepSize)
          xIndex = FIND( x > xp )
          yIndex = FIND( y > yp )
          z = elevationMatrix(LAST(xIndex), LAST(yIndex))
          SAVE  xp, yp, z
          DECREAMENT numberOfCells BY 1
          INCREAMENT stepSize BY cellLength
       END
END
EXIT
```

2.4 Material Input Operations Simulation Tool

In this stage, the execution of the operation following the tested driving angle is simulated using a developed model by Hameed et al. [7]. The object oriented simulation model regards the material input operations with capacity constraints, where a quantity of a "commodity" is transported by the machine and is distributed in the field area (e.g. the case of the organic fertilizing application). In the case of material input operations, a number of routes are required since a full load carried by the application unit is generally not sufficient for full area coverage of the field. A "route" consists of part operations including filling the tanker at a location out of the field and driving from that location to the position where the application is resumed, applying the carried material to the field, and driving back to the re-filling location. These activities involve a number of non-productive in-field transports with either full (in the case of travelling from the refilling location and then back to the vehicles resuming position) or empty (the opposite of the previous explanation above) tanker. All these in-field transports are directly affected by the driving angle and have to be included in the estimation of the total energy requirements. The input to the simulation tool includes the 2D geometrical representation of the field (provided by the tool described in Section 2.2), a number of operation-specific information, i.e. application rate, dosage of the material, average speeds (working speed, turning speed, and in-field transport speed), and machinery-specific information, i.e. minimum turning radius, working width, and tank capacity. The output of the simulation model provides the sequence that the vehicle traverses the waypoints with which has been defined in the 3D representation stage and the load carried by the vehicle at the individual waypoints in both the case of applying the material and in the case of the associated in-field transports.

2.5 Energy Requirements Estimation Model

In order to model the agricultural vehicle energy consumption as a function of the inclination of the field terrain, the case of the injector system for organic fertilizer was used. Specifically, the estimation of the required power was based on the following parametric equation introduced Fröba and Funk by [3]:

$$\begin{aligned} P = {} & (p_1 + v \cdot w \cdot p_2) + \left(p_3 + d \cdot v^2 \cdot p_4\right) w \\ & + (0.115 M \cdot v \cdot a/3600) + P_{air} \\ & + (g \cdot m \cdot v \cdot r_{rc}/1800) \end{aligned} \tag{1}$$

where P is the required power (kW), v is the vehicle speed (km/h), w is the working width of the injector (m), d is the working depth (cm), M is the total vehicle and implement mass including the tank load, m is the vehicle and implement mass, (kg), a is the inclination of the terrain (%), g is the gravitational acceleration (9.81 m/s^2), P_{air} is the total power account for air conditioner and compressors (kW), r_{rc} is the rolling resistance coefficient (r_{rc} equals 0.06 for good surface conditions, 0.12 for medium surface conditions, and 0.25 for bad surface conditions), p_1 and p_2 are pump constants ($p_1 = -0.2683$ and $p_2 = 0.06775$), and p_3 and p_4 are injector factors (i.e., $p_3 = 4.55752$ and $p_4 = 0.03141$). Equation 1 is used to estimate the power required by a tractional unit pulling an injector traversing each segment of the generated 3D representation of the field according to the following process.

Let $T = \{1,2,3,\ldots\}$ be the set of the field-work tracks generated by the 2D representation process. Each track is divided into a number of segments n_i, $i \in T$ according to the 3D representation process. In each of the above mentioned segments, an inclination $a^i_j, i \in T, j = 1, \ldots n_i$ is allocated (in the 3D representation process). To calculate the inclination in a specific segment of a track, the change in elevation between two sequential cells in the direction of the track is divided by the length of the cell edge. In the case of time-depended loads in each segment, a mass value $M^i_j = m + l^i_j, i \in T, j = 1, \ldots, n_i$ is allocated and this equals the summation of the machinery (tractor + implement) mass, m (kg), and the load mass ($l^i_j, i \in T, j = 1, \ldots, n_i$) (this value is provided by the simulation tool output). Consequently, the required power for driving over

each individual segment can be obtained using the following equation:

$$P_j^i = \begin{cases} (p_1 + v.w.p_2) + \left(i_1 + d.v^2.i_2\right) w + \left(0.115.\left[m + l_j^i\right].v.a_j^i/3600\right) + P_{air} + (g.m.v.r_{rc}/1800), & \text{if } a_j^i > 0 \\ (p_1 + v.w.p_2) + \left(i_1 + d.v^2.i_2\right) w + P_{air} + \left(g.v.r_{rc}/1800\right), & \text{otherwise} \end{cases} \quad (2)$$

The tank load for each segment is obtained using the equation:

$$\begin{aligned} l_1^1 &= C \\ l_1^i &= l_{n_{i-1}}^{i-1} - r.w.d_1^i, i \in T \setminus \{1\} \\ l_j^i &= l_{j-1}^i - r.w.d_j^i, i \in T,\ j = 2, \ldots, n_i \end{aligned} \quad (3)$$

where r is the application rate in (kg/m^2), d_j^i is the segment length, and C is the tank capacity (kg).

The energy model Eq. 2 is a simplification ignoring the full effect of driving in a negative slope. As it can be seen in the case of the negative slope the energy requirements have been assumed to be equal to the one while driving in zero slope. Although that this assumption has no effect in the optimality of the solution, the resulted values of the energy requirements are not true values but higher and have to be regarded as the output of the objective function of the optimization problem and not as the real energy requirements of the system.

The energy required for traversing each individual segment is obtained using:

$$E_j^i = 3.6\frac{P_j^i \cdot d_j^i}{v} \quad (4)$$

The total energy required for covering the main field body is then estimated as:

$$E = \sum_{i=1}^{|T|}\left(\sum_{j=1}^{n_i} E_j^i\right) \quad (5)$$

As mentioned, in each route executed by the vehicle an empty tanker in-field transport and a full-tanker in-field transport are involved. For each of these in-field transports, the simulation tool provides the sequence of the way points. The energy requirements for each individual segment traversed by the vehicle in an in-field transport is estimated using Eq. 2 where for the case of an empty tanker the total vehicle mass equals m, while in the case of a full-load tanker equals $m + c$, where c is the tanker capacity. The total energy requirements for the in-field transports equal:

$$E_{tr} = \sum_{i=1}^{k}\left(E_i^e + E_i^f\right) \quad (6)$$

where k denotes the number of routes and E_i^e and E_i^f are the total direct energy requirements for the empty tanker and the full-loaded tanker, respectively, in-field transports during route $i \in \{1, \ldots k\}$.

In the optimization problem, the driving angle which minimizes the total energy consumed in covering field area and in the associated in-field transportations is found. The objective function is given as follows:

$$\min_{\vartheta \to \vartheta^*} (E + E_{tr}) \quad (7)$$

where $\vartheta \in [0°, 180°]$ is the driving angle and ϑ^* is the optimum driving angle which minimizes the total energy consumption. The model has been implemented in the MATLAB® programming environment.

3 Case Studies

3.1 The Experimental Fields

Two experimental fields, referred to as field A and field B, were used for demonstrating the func-

tionality of the developed approach. Figure 4a shows the satellite image of the experimental field A (+56° 30′ 25.64″ N, +9° 35′ 11.45″ E) which has an area of 11.24 ha (112,416.45 m^2). The minimum, maximum and average elevations on this field are 20.89 m, 42.96 m, and 32.88 m, respectively. The 3D surface area of field A, the contour view of the field's elevation model (i.e., DEM) and two elevation profiles of Field A are shown also in Fig. 4. Figure 5 shows the satellite image of the experimental field B (+56° 30′ 48.10″ N, +9° 34′ 15.61″ E) which has an area of 21.22 ha (212,168.67 m^2). The minimum, maximum, and average elevations on this field are 18.68 m, 42.96 m, and 35.77 m, respectively. The 3D surface area of field B, the contour view of the field's elevation model (i.e., DEM) and two elevation profiles of field B are shown also in Fig. 5.

3.2 Results and Discussion

3.2.1 2D/3D GA-Based Approach

At the first stage, the driving angle for experimental field A is optimized using a binary coded GA of 0.5 crossover probability, 0.2 mutation probability and for a vehicle of an operating width of 9 m and a minimum turning radius of 7.5 m derived at an average speed of 10 km/h in field-work tracks, 5 km/h in pi-turning type and 2.5 km/h in omega-turning type (for more details see [7]). Two different population sizes are used to assess the performance of the driving angle optimization algorithm over 2D representation. The optimized driving angles for a GA of 40 and 150 chromosomes in population are found to be 99.36° and 99.15°, respectively, and this solution is obtained in 0.58 and 1.43 min, respectively, as it is shown in

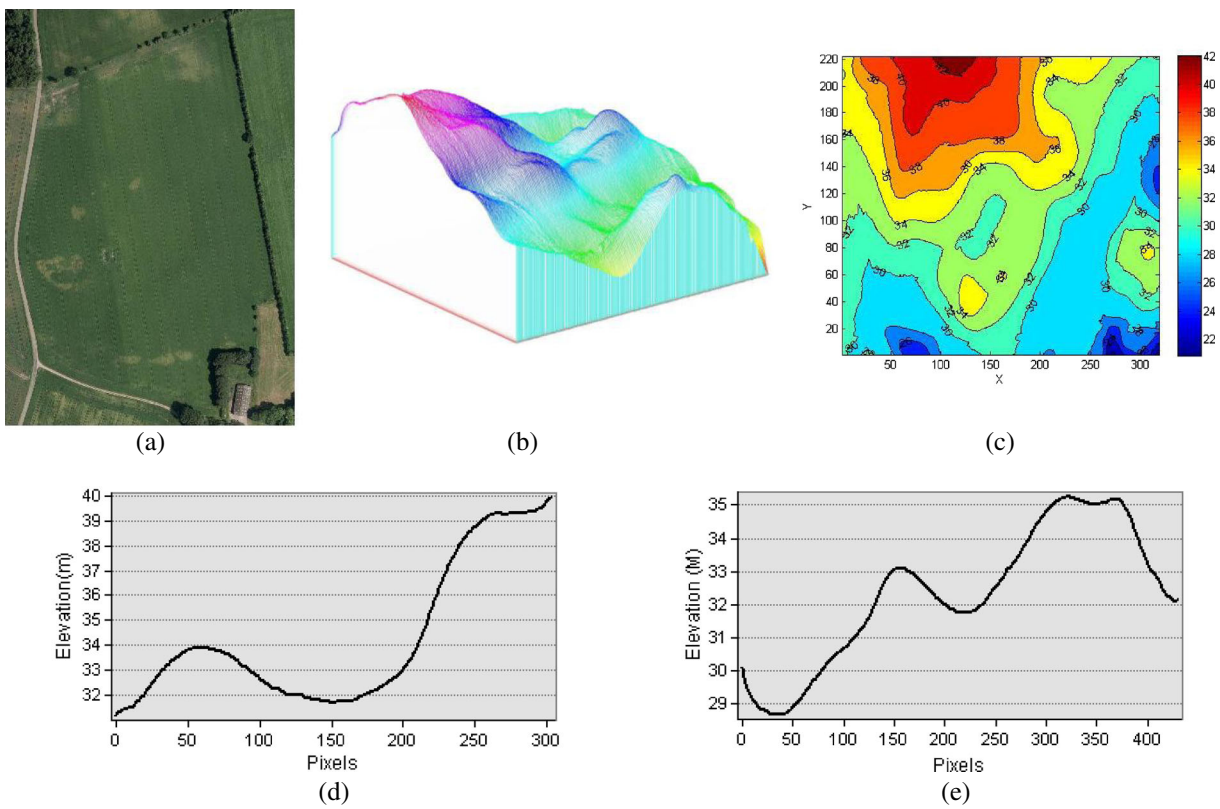

Fig. 4 Experimental Field A: Satellite image (**a**), 3D surface view (**b**), contour view based on the DEM information (**c**), elevation profile from west (W) towards east (E) (**d**), and elevation profile from north (N) towards south (S) (**e**)

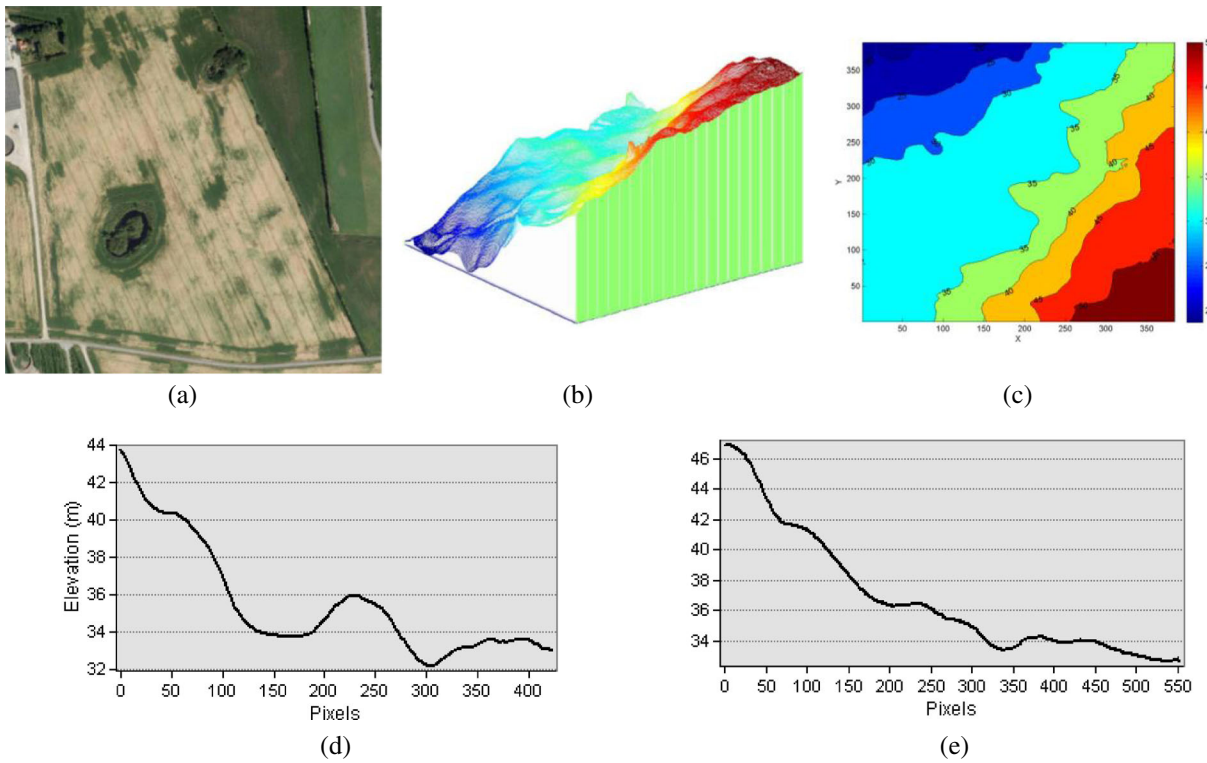

Fig. 5 Experimental Field B: Satellite image (**a**), 3D surface view (**b**), contour view based on the DEM information (**c**), elevation profile from west (W) towards east (E) (**d**), and elevation profile from north (N) towards south (S) (**e**)

Table 2. A more accurate solution can be obtained (i.e., in terms of less non-working distance) for a larger population size but at the cost of the computing time. The driving angle is optimized over 3D field representation using the above GA where an optimized driving angle of 100° is obtained in 23.64 min as it is shown in Table 2.

Table 3 shows a comparison between some empirical driving angles and the optimized driving angles over 2D and 3D field terrains. The total track length for the 2D and 3D optimized driving angle of the coverage plan are found to be 11852.94 and 11992.5 m, respectively. Only 139.56 m difference in track length is verified which has an insignificant impact on the optimized solution, however, traversing the field at an angle of 100° results in covering the same field area using 32 tracks compared to 33 tracks in case of 99° and hence less operational time due to a one less turning over the headland area. The 2D field representation for a driving angle of 100° is shown in Fig. 6a while its 3D field representation is shown in Fig. 6b. From the table, it is obvious that minimizing the non-working distance results

Table 2 Optimized driving angle over 2D and 3D optimization (^{2D} refers to the optimal value obtained in 2D and ^{3D} refers to the optimal value obtained in 3D)

Run number	Population size (# of chromosomes)	Optimized angle (°)	Computing time (min)	Cost (nonworking distance m)
1^{2D}	40	99.36	0.58	1545.18
2^{2D}	150	99.15	1.43	1541.33
3^{3D}	150	100.0	23.64	1564.24

Table 3 A Comparison between some empirical and the optimized driving angles (^{2D} refers to the optimal value obtained in 2D and ^{3D} refers to the optimal value obtained in 3D) of experimental field A

Driving angle (°)	Number of rows	Rows length (m)	Nonworking distance (m)	Operational time (h)
0.0	53	11858.33	2493.69	2.10
45.0	48	11958.40	2453.22	2.05
90.0	35	11854.44	4290.14	2.05
99.15^{2D}	33	11852.94	1541.32	1.75
100.0^{3D}	32	11992.50	1564.24	1.72
135.0	50	11846.44	2540.22	2.07

in a significant reduction in total operational time by about −15.4 % from the average operational time of the four selected empirical driving angles which is 2.07 h. the reduced operational time can be easily transformed into economic savings in terms of operational cost and fuel consumption. In addition to the economic savings, there is the environmental impact represented in the reduced emissions of CO_2 and other greenhouse gases as a result of the reduced combustion of fossil fuels. Also, there is the increased yield as a result of the reduced driving over headland area and hence the reduced degradation of soil fertility due to soil compaction and over driving.

An energy model is used to estimates fuel consumed per each track (l/m^2) by a vehicle/tractor for a good roadway conditions driving through the field tracks represented in 3D from one end to the other end (i.e., forward direction) and vice versa (i.e., return direction), and by driving through the flat field tracks (i.e., represented in 2D with zero inclination) are shown in Fig. 7. The difference in fuel consumption in both forward and return directions emphasis the impact of elevation profile,

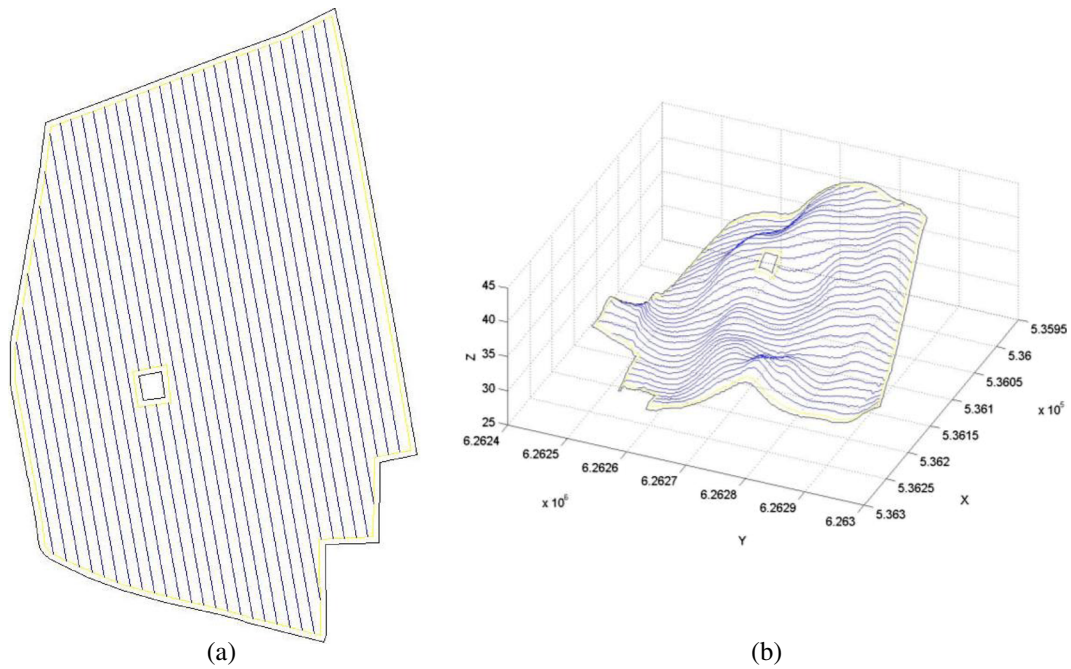

(a) (b)

Fig. 6 Driving patterns of the first experimental field A for a 3D optimized driving angle of 100°: **a** 2D driving pattern for optimized driving angle, **b** 3D terrain driving pattern

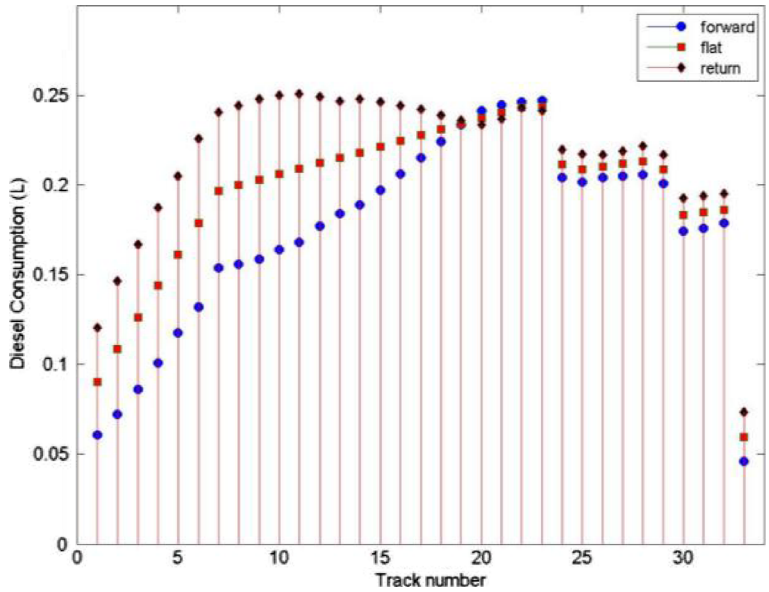

Fig. 7 Diesel requirements (l) to cover field tracks of experimental field A from both sides in 3D (forward and return direction) and 2D (flat) for good roadway conditions

shown in Fig. 4d and e, on fuel consumption where the field surface is ascending in the west-to-east (WE) and north-to-south (NS) directions.

A GA is used to find a compromised sequence of tracks which minimizes the total fuel consumption such as a vehicle travels in a track in one direction and returns back in the next track in the reverse direction, as it is shown in Table 4. From Table 4, a significant reduction in the total fuel consumption in the range of −8.06 % can be achieved in the case of applying the optimized track sequence over 3D terrain.

The driving angle for experimental field B is optimized over 2D field representation using a binary GA with the same parameters and conditions used above for experimental field A except that the proposed vehicle/tractor has a new implement of 18 m working width. The optimized driving angles for two different population sizes are shown in Table 5. A minimum non-working distance of 900.67 m is obtained for a driving angle of 111.02°. For this field, it is obvious that increasing the population size does not improve the solution quality. In addition, optimizing the driving angle over 3D field representation which is found to be 90° and is obtained in 14.24 min did not provide a better solution, as it is shown in Table 5.

Table 6 shows a comparison between some empirical driving angles and the optimized driving angles over 2D and 3D field terrains. The total track length for the 2D and 3D optimized driving angle of the coverage plan are found to be 11445.71 and 12729.28 m, respectively. Due to the complex terrain of the field, 11445.71 m difference in track length is verified which has a significant impact on the optimized solution, however, traversing the field at an angle of 111°

Table 4 Optimized/compromised sequence of tracks of experimental field A for good roadway conditions (first track is forward)

Optimized sequence of tracks											Total fuel consumption (l)		
											2D	3D	
											default sequence	Default sequence	GA optimized
[5	21	14	23	7	27	33	28	11	31	10	6.45	6.38	5.93
18	12	26	9	30	6	19	15	22	1	29			
13	25	4	24	3	20	16	17	2	32	8]			

Table 5 Optimized driving angle for two different population sizes of the second field

Run number	Population size (# of chromosomes)	Optimized angle (°)	Computing time (min)	Cost (nonworking distance m)
1^{2D}	40	111.02	0.59	900.67
2^{2D}	150	111.22	2.16	902.45
3^{3D}	150	90.0	14.24	3761.53

results in covering the same field area using 25 tracks compared to 31 tracks in case of 90° and hence less operational time due to 12 less turning over the headland area. The 2D field representation for a driving angle of 111.02° is shown in Fig. 8a while its 3D field representation is shown in Fig. 8b. From the table, it is obvious that minimizing the non-working distance results in a significant reduction in total operational time by about −10.96 % from the average operational time of the four selected empirical driving angles which is 1.46 h. the reduced operational time can be easily transformed into economic savings in terms of operational cost and fuel consumption. In addition to the economic savings, there is the environmental impact represented in the reduced emissions of CO_2 and other greenhouse gases as a result of the reduced combustion of fossil fuels. Also, there is the increased yield as a result of the reduced driving over headland area and hence the reduced degradation of soil fertility due to soil compaction and over driving.

An energy model is used to estimates fuel consumed per each track (l/m^2) by a vehicle/tractor for a good roadway conditions driving through the field tracks represented in 3D from one end to the other end (i.e., forward direction) and vice versa (i.e., return direction), and by driving through the flat field tracks (i.e., represented in 2D with zero inclination) are shown in Fig. 9. The difference in fuel consumption in both forward and return directions emphasis the impact of elevation profile, shown in Fig. 5d and e, on fuel consumption where the field surface is descending in the west-to-east (WE) and north-to-south (NS) directions.

A GA is used to find a compromised sequence of tracks which minimizes the total fuel consumption such as a vehicle travels in a track in one direction and returns back in the next track in the reverse direction, as it is shown in Table 7. From Table 4, a significant reduction in the total fuel consumption in the range of −3.24 % can be achieved in the case of applying the optimized track sequence over 3D terrain.

3.2.2 Enumeration Approach

The inputs for the simulated operations for both field A and field B included a machinery system involving a tractor and an organic fertilizer injector of a weight of 10.5 t. Four scenarios, in terms of different working width and tanker capacity combinations, were simulated, namely, scenario 1 (S1): a 6 m working width with a 15 t tanker capacity, scenario 2 (S2): a 6 m working width with a 25 t tanker capacity, scenario 3 (S3): a 9 m working width with a 25 t tanker capacity, scenario 4 (S4): a 9 m working width with a 35 t tanker capacity.. The assessed working speed was 8 km/h, and the turning speed was 5 km/h. Finally,

Table 6 Comparison between some empirical and optimized driving angles of experimental field B (^{2D} refers to the optimal value obtained in 2D and ^{3D} refers to the optimal value obtained in 3D)

Driving angle (°)	Number of rows	Rows length (m)	Nonworking distance (m)	Operational time (h)
0.0	31	11333.03	1277.12	1.34
45.0	40	11256.48	1642.73	1.39
90.0^{3D}	31	12729.28	3761.53	1.73
111.02^{2D}	25	11445.71	900.68	1.30
135.0	31	11335.65	1436.58	1.36

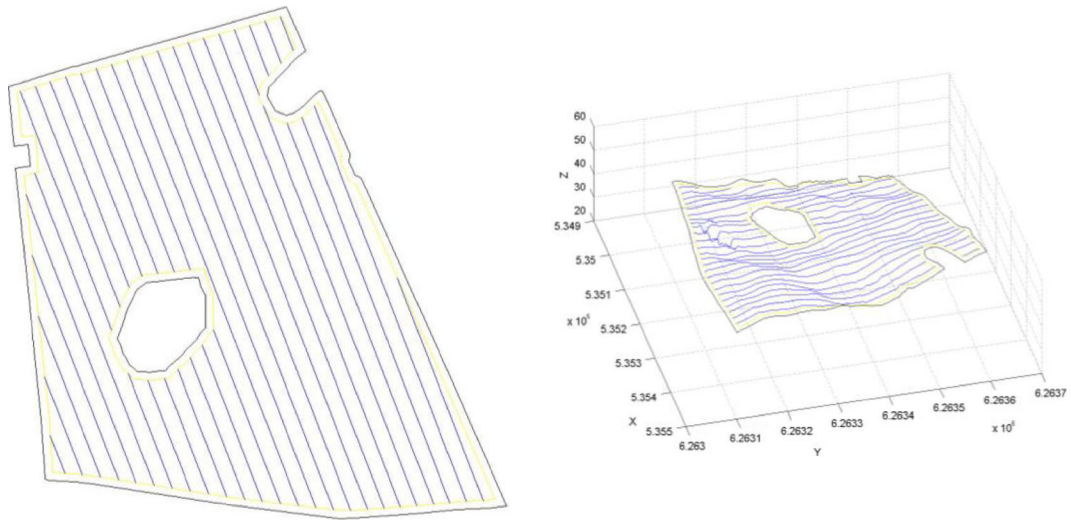

Fig. 8 Driving pattern of the second experimental field for a working width of 18 m and for an optimized angle of 111.02°: **a** optimized 2D driving pattern, **b** optimized 3D terrain driving pattern

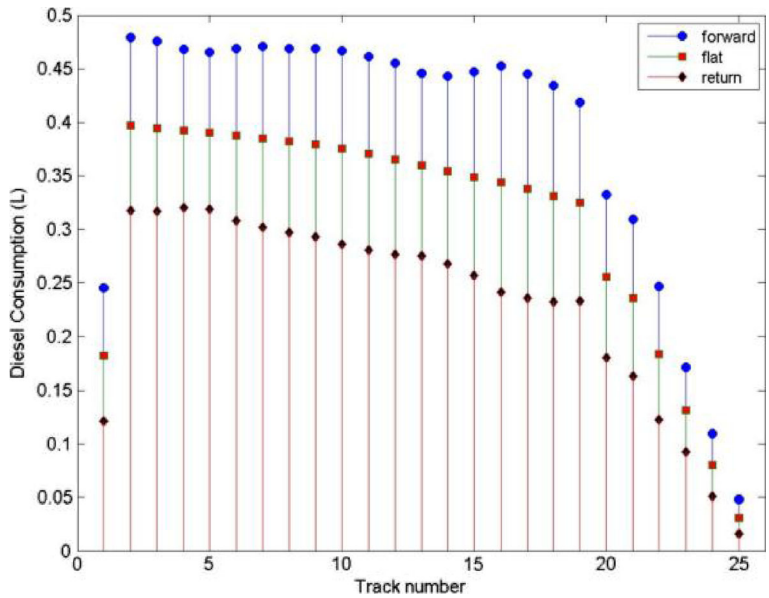

Fig. 9 Diesel requirements (l) to cover field tracks of experimental field B from both sides in 3D (forward and return direction) and 2D (flat) for good roadway conditions

Table 7 Optimized/compromised sequence of tracks of experimental field B over 3D field representation for good roadway conditions (first track is forward)

Optimized sequence of tracks	Total fuel consumption (l)		
	2D	3D	
	default sequence	Default sequence	GA optimized
[7 17 24 14 25 19 22 10 3 15 2 11 20 12 1 18 5 16 6 9 21 8 4 13 23]	7.72	7.71	7.47

Table 8 Output operational parameters for the optimized driving angle for the experimental fields

	Field A				Field B			
Scenario	S1	S2	S3	S4	S1	S2	S3	S4
Operating width (m)	6	6	9	9	6	6	9	9
Tank capacity (t)	15	25	25	35	15	25	25	35
Optimal angle (°)	100	165	100	165	172	172	36	36
Number of tracks	49	79	32	52	94	94	78	78
Refills	36.0	22.0	22.0	15.0	72.0	43.0	43.0	31.0
Energy requirements for application (MJ)	23,555	19,916	14,812	12,403	52,998	38,749	29,834	24,986
Energy requirements for full tanker transport (MJ)	7,994	5,889	5,938	4,407	39,115	22,373	23,836	17,737
Energy requirements for empty tanker transport (MJ)	17,630	9,561	10,799	6,447	46,608	44,113	28,441	23,496

the application rate was assessed 50 t/ha, refilling time was 10 min, and good surface conditions (i.e., for good roadway conditions $r_{rc} = 0.06$) were assumed. The results of the method applied in the experimental fields are listed in Table 8.

For field A, the optimized driving angles were found to be 100° for scenarios S1 and S3 and 165° for scenarios S2 and S4. The 3D configuration of the field work tracks for these two driving angles are presented in Fig. 10. Figure 11 presents the energy requirements for the different in-field part operations (i.e. full tanker transport, empty tanker transport, and travelled distance during the application phase which is in this paper called operational energy) as a function of the tested driving angles. Respectively, in the case of field B, the optimized angles were found to be 172° for the scenarios S1 and S2, and 36° for scenarios S3

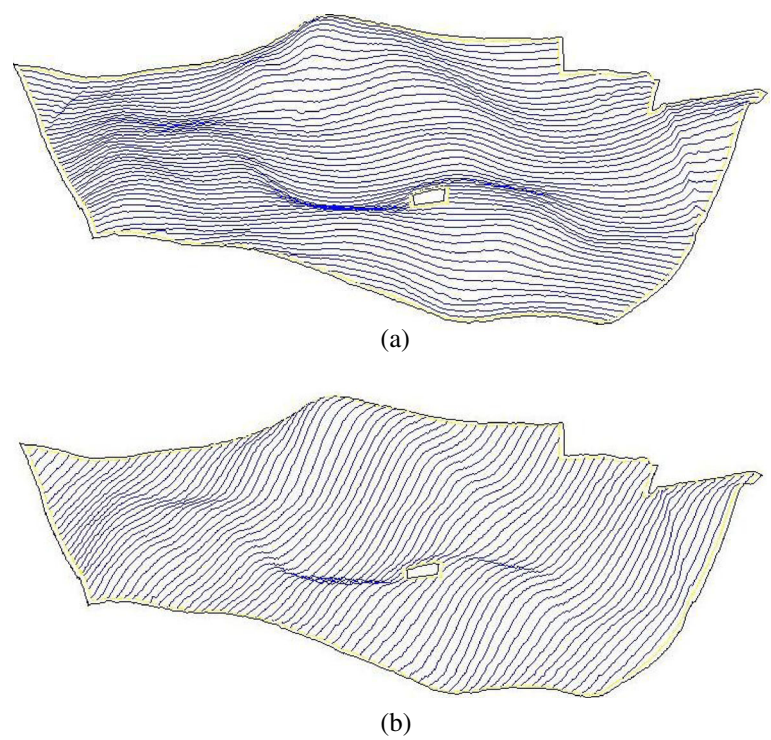

Fig. 10 Field-work tracks configuration for experimental field A for the optimized driving direction for S1 and S3 **a** 100°, and for S2 and S4 **b** 165°

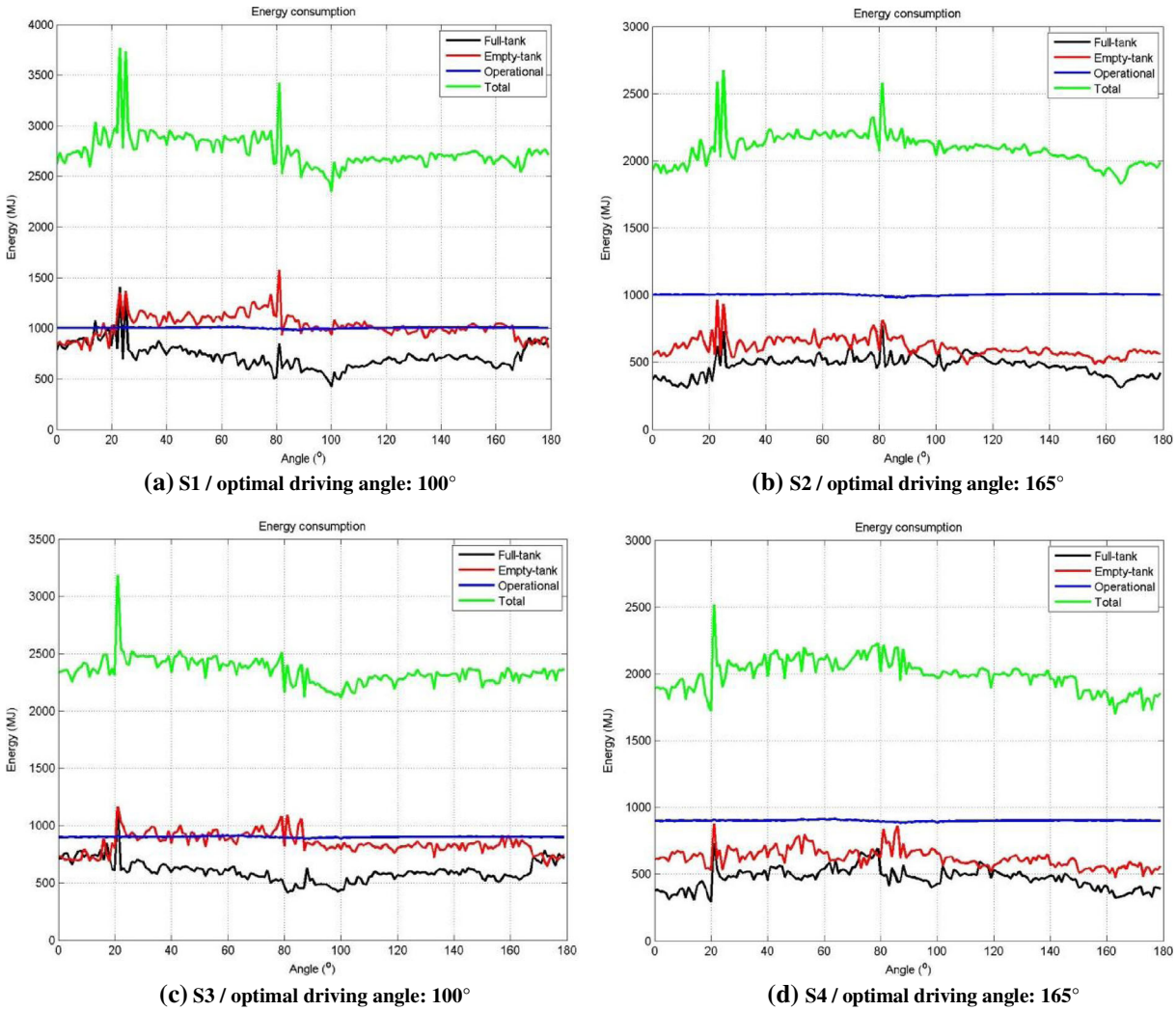

(a) S1 / optimal driving angle: 100°

(b) S2 / optimal driving angle: 165°

(c) S3 / optimal driving angle: 100°

(d) S4 / optimal driving angle: 165°

Fig. 11 Energy consumed in in-field activities for the different driving angles for the experimental field A

and S4. The 3D configuration of the field work tracks on field B for these two driving angles are presented in Fig. 12, and the energy requirements as a function of the driving angle are presented in Fig. 13.

The computational time for the four scenarios S1, S2, S3, and S4 were 130.2 min, 127.3 min, 66.0 min, and 60.7 min, respectively, for field A, and 380.1 min, 274.7 min, 184.7 min, and 189.4 min, respectively, for field B. The high computational requirements are caused by the exhaustive search among all possible integer values of driving angles between 1° and 180° which result in 179 executions of the object oriented simulation for the operation. It is obvious that the computational time increases with the number of the travelled distance of the machine for covering the field area which is a function of the field area (for all scenarios the computational time for field B is higher than the corresponding computational time for field A) and of the working width (for both field A and field B the computational times for scenarios S1 and S2 are higher than the computational times for scenarios S3 and S4, since a longer working width results in less field work tracks created or equivalently in shorter travelled distance

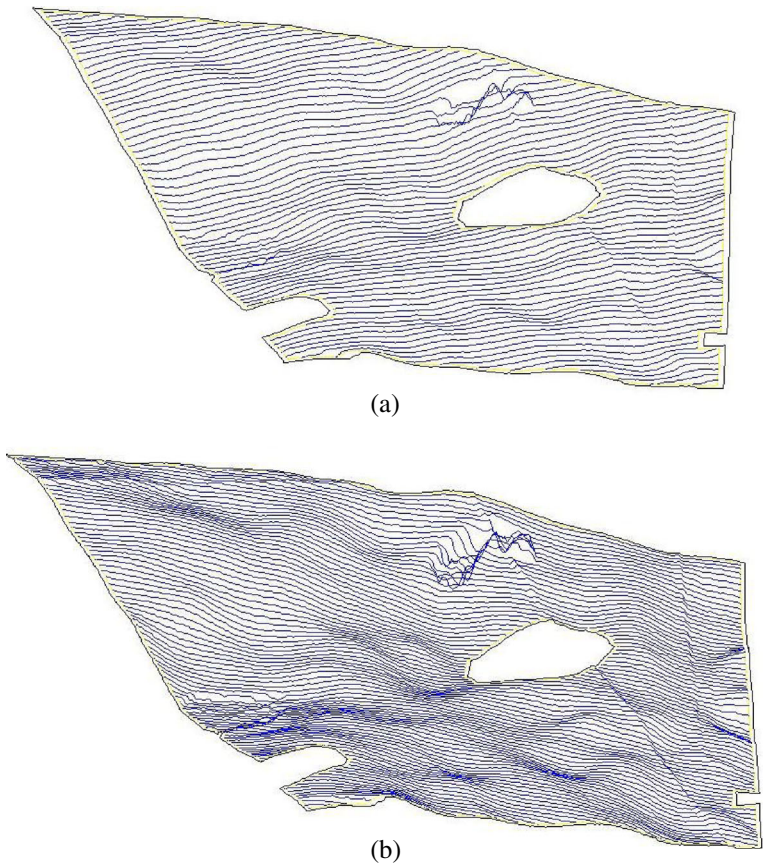

Fig. 12 Field-work tracks configuration for experimental field B for the optimized driving direction for S1 and S2 **a** 172°, and for S2 and S4 **b** 36°

realized). In any case, the high computational requirements of the presented system prohibits its application as an on-line (e.g. on-board) tool and its utility is restricted to an off-line decision making tool.

In order to examine the importance of the optimizing of the driving angle in the 3D space instead of in the 2D space, all the simulation experiments were also executed assuming plane field area (the z-coordinates values in DEM files were replaced by zero). The resulted optimized driving angles for optimizing in the 2D space were 100° for all scenarios in field A, and 4° for S1 and S2, and 114° for S3, and S4 in field B. There is a coincidence in the solution in both 2D and 3D spaces in the case of S1 and S3, field A. Table 8 lists the energy and operational time requirements for the execution of the operation (in the 3D space) following the driving angle that results from the optimization in 2D space and 3D space. The reduction in the energy requirements when the driving angle is optimized by taking into account the 3D configuration of the field area is 6.4 % for field A (ranged between 0 in S1 and 13.6 in S2) and 6.7 % for field B (ranged between 6.0 % in S1 and 6.8 % in S2) resulting in a total average of 6.5 % for all cases.

Regarding the operational time, as it can be seen in Table 9, the optimization under the criterion of minimizing the energy requirements can have a negative impact. In the case of field A, there is an increase in the operational time of 8.7 % in S2 and of 6.7 % in S2 (3.8 % increase in average for all scenarios in field A), while in the case of field B there is an increase of 10 % in S1 and of 2.1 % in S2 (3.9 % reduction in average for all scenarios in field B).

Based on the previous, the implementation of a multiple-criteria optimization is an objective for future research where the energy requirements and operational time requirements will be

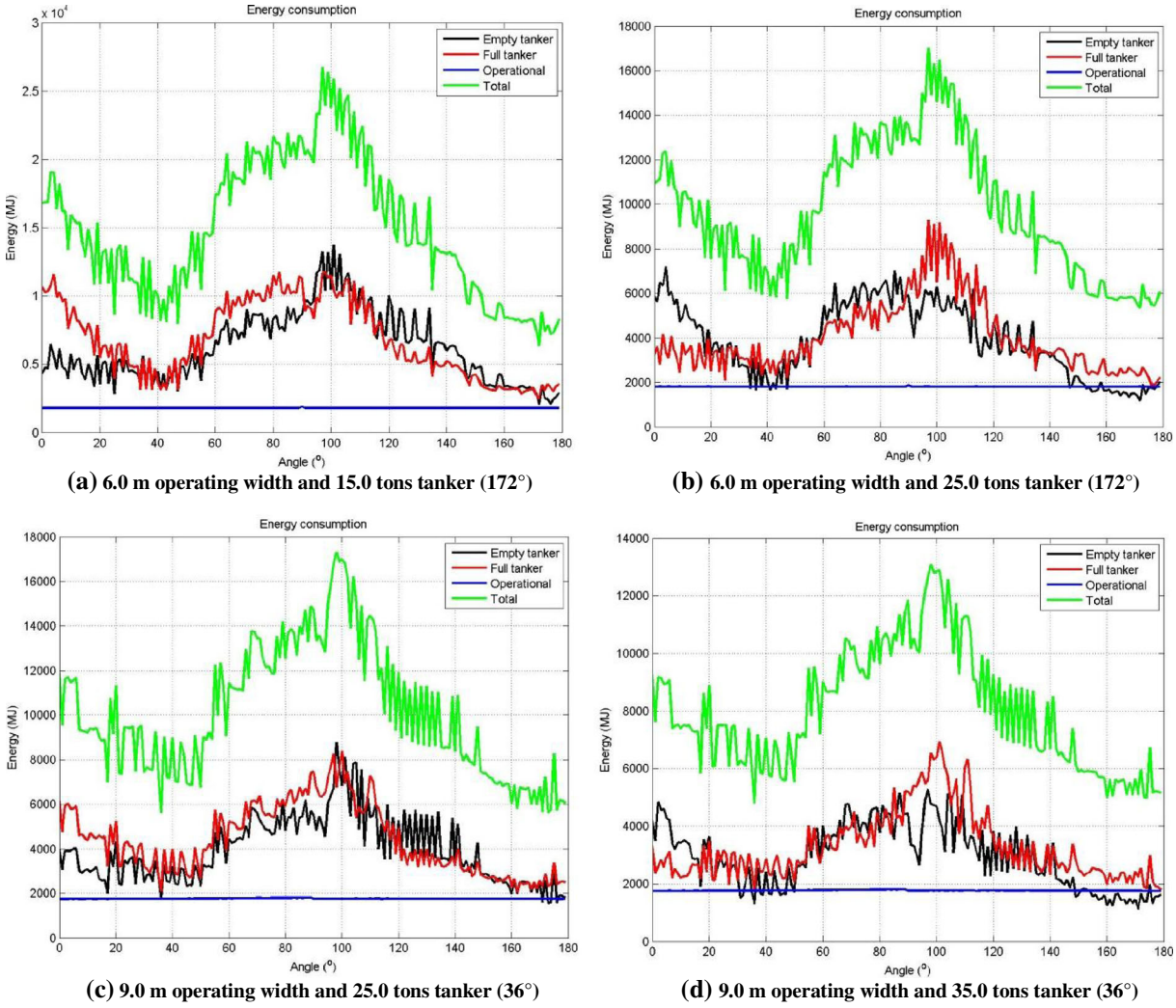

(a) 6.0 m operating width and 15.0 tons tanker (172°)

(b) 6.0 m operating width and 25.0 tons tanker (172°)

(c) 9.0 m operating width and 25.0 tons tanker (36°)

(d) 9.0 m operating width and 35.0 tons tanker (36°)

Fig. 13 Energy consumed in in-field activities for the different driving angles for the experimental field B

both taking into consideration. Another future research objective is a two-step optimization approach where beyond the driving angle, the traversal sequence of the tracks (default patterns) will be a second decision variable as it is shown in the previous approach.

Table 9 Comparison of energy and operational time requirements between the simulated operations when optimizing under 2D and 3D conditions

		Field A				Field B			
		S1	S2	S3	S4	S1	S2	S3	S4
Total energy requirements (MJ)	2D	2354	2113	2086	1937	6941	5898	5998	5129
	3D		1827		1701	6493	5471	5610	4798
	Discrepancy[a] (%)	0	13.6	0	12.2	6.0	6.8	6.5	6.5
Operational time (h)	2D	2.9	2.3	1.9	1.5	6.0	4.7	4.3	3.6
	3D		2.5		1.6	6.6	4.8	3.7	3.1
	Discrepancy[a] (%)	0	−8.7	0	−6.7	−10.0	−2.1	14.0	13.9

[a](2D value–3D value)/2D value) × 100 %

4 Conclusions

Optimized terrain field coverage path planning approach is developed and an approach for a multiple-objective optimal coverage planning approach for field operations is presented. The analysis of different coverage costs on 2D and 3D terrains was conducted. A significant reduction in operational time in the range of 10–15 % and can be achieved. The fuel consumption can be further reduced by optimizing the track sequence over 3D field terrain. The combination of a modelling approach for the 3D geometrical representation of the field area and an object oriented simulation tool for field operations under capacity constraints can provide the optimized driving angle direction for traversing the parallel field-work tracks for an agricultural vehicle caring out this type of operations, under the criterion of minimized direct energy requirements. The problem presents itself like a typical decision making task under the uncertainty problem and the results show that the inclusion of additional information, here in the form of field inclinations, improves the utility of the process. Specifically and based on the results from two case study fields, it was shown that the reduction in the energy requirements when the driving angle is optimized by taking into account the 3D configuration of the field area was 6.5 % as an average for all the examined scenarios, compared to the case when the applied driving angle is optimized assuming even field areas. Reduced total energy requirements are subsequently equivalent to reduced fuel consumption and direct CO_2 emissions. Nevertheless, the objective of minimizing energy requirements could result in coverage plans that require increased operational time and potentially add to increased cost.

References

1. Bochtis, D.D., Vougioukas, S.: Minimising the non-working distance travelled by machines operating in a headland field pattern. Biosyst. Eng. **101**(1), 1–12 (2008)
2. FAO: energy smart food for people and climate. Food and Agriculture Organization of the United Nations, Rome, pp. 1–66. Available at http://www.fao.org/docrep/014/i2454e/i2454e00.pdf (2011)
3. Fröba, N., Funk, M.: Teilzeitspezifische Dieselbedarfskalkulation bei Arbeiten in der Außenwirtschaft. KTBL-Arbeitsblatt: Landtechnik und Pflanzenbau Nr. 0255 'Benötigte Traktormotornennleistung bei landwirtschaftlichen Arbeiten' (N. Fröba, 1995) (in Germany) (1995)
4. Hameed, I.A., Bochtis, D.D., Sørensen, C.G.: Driving angle and track sequence optimization for operational path planning using genetic algorithms. Appl. Eng. Agric. **27**(6), 1077–1086 (2011)
5. Hameed, I.A., Bochtis, D.D., Sørensen, C.G.: An optimized field coverage planning approach for navigation of agricultural robots in fields involving obstacle areas. Int. J. Adv. Robotic Syst. **10**, 1–9 (2013)
6. Hameed, I.A., Bochtis, D.D., Sørensen, C.G., Nøremark, M.: Automated generation of guidance lines for operational field planning. Biosyst. Eng. **107**(4), 294–306 (2010)
7. Hameed, I.A., Bochtis, D.D., Sørensen, C.G., Vougioukas, S.: An object oriented model for simulating agricultural in-field machinery activities. Comput. Electron. Agr. **81**(1), 24–32 (2012)
8. Hameed, I.A., Bochtis, D.D., Sørensen, C.G., Jensen, A.L., Larsen, R.: Optimized driving direction based on a three-dimensional field representation. Comput. Electron. Agr. **91**, 145–153 (2013)
9. Jin, J., Tang, L.: Optimal coverage path planning for arable farming on 2D surfaces. Trans. ASABE **53**(1), 283–295 (2010)
10. Jin, J., Tang, L.: Coverage path planning on three-dimensional terrain for arable farming. J. Field Robot. **28**(3), 424–440 (2011)
11. Oksanen, T., Visala, A.: Coverage path planning algorithms for agricultural field machines. J. Field Robot. **26**(8), 651–668 (2009)
12. Stombaugh, T., Koostra, K.B., Dillon, R.C., Mueller, G.T., Pike, C.A: Implications of Topography on Field Coverage When Using GPS-Based Guidance. University of Kentucky (2009)
13. Sulebak, J.R.: Applications of Digital Elevation Models. Department of Geographic Information Technology. SINTEF Applied Mathematics, Oslo, Norway (2000)
14. Tavares, G., Zsigraiova, Z., Semiao, V., Carvalho, M.G.: Optimization of MSW collection routes for minimum fuel consumption using 3D GIS modelling. Waste Manage. **29**(3), 1176–1185 (2009)
15. Warwick H.R.I.: Ac0401: Direct Energy Use in Agriculture: Opportunities for Reducing Fossil Fuel Inputs. University of Warwick, Warwick (2007)